RSC Advances

ROYAL SOCIETY OF CHEMISTRY

www.rsc.org/advances

RSC Advances

RSCPublishing

COMMUNICATION

Cite this: DOI: 10.1039/xoxxoooooox

Ammonia-Assistant Epitaxial Assembly of Cu_2O@Ag Yolk-Shell and Ag Cage

Received ooth March 2014,
Accepted ooth March 2014

DOI: 10.1039/xoxxoooooox

www.rsc.org/advances

Jiqiao Zhang, Cui Zhang, and Shuangxi Liu*

Effective in site redox, epitaxial assembly of Cu_2O@Ag and Ag cage in high yield respectively were acquired through introducing $[Ag(NH_3)_2]^+$ ions to the dispersed Cu_2O suspension under visible-light irradiation, without any other chemical required. The $[Ag(NH_3)_2]^+$ ions play a critical role in the Ag-shell growth and keep morphologies similar to that of Cu_2O template.

Metal/metal oxide semiconductor that can manifest distinct reactivity from the initial, as-prepared materials, have gained increasing attention owing to their promising applications in catalysis, delivery vehicles, gas sensors and theory researches. [1-11] Especially, IB group metals loaded oxidation semiconductors have been investigated extensively. [12-22] However, organic agents were required whereas causing an organic layer existed between the metal particles and the supporting semiconductors in previous proposals. [23-27] As a result, organic layer would worsen the properties of the composites. As a p-type semiconductor with a band gap of 2.17eV, Cu_2O is a kind of promising material with potential applications in gas sensors, catalysis, solar-energy conversion, lithium-ion batteries, and water splitting. [28-32] So far, to overcome these disadvantages, several complicated techniques including sputtering deposition, chemical-deposition, hydro-thermal method, photochemical deposition have been used to prepare clean Ag/Cu_2O composite, which combined with charge-extraction layers and endowed "hot spot" exhibit a sharply increase in practical applications. [33-35] A facile method in situ redox reaction is to be desired that metal particle directly form over a semiconductor substrate, without foreign reducing agents, stabilizing molecules, organics holding interlink-group.

Our inspiration came up with the following idea sparkled by Xi and Wang *et al.*. [36] Dissolvable $[Cu(NH_3)_4]^{2+}$ can be obtained through adding Cu_2O to ammonia solution, so we added aqueous ammonia to silver nitrate solution for forming $[Ag(NH_3)_2]^+$ complex then adding $[Ag(NH_3)_2]^+$ complex to the dispersed Cu_2O suspension. Because $[Ag(NH_3)_2]^+$ ions adhere to the surface of Cu_2O, Cu_2O act with $(NH_4)^+$ as Equ. 1. Because Cu^+ ions released from Cu_2O has a weak reducing power in low valance state and Cu_2O triggers electron and hole under visible-light irradiation, Cu_2O@Ag yolk-shell and Ag cage can be prepared through an in situ redox, as Equ. 2-5, epitaxial assembly reaction between weakly reductive Cu_2O and $[Ag(NH_3)_2]^+$ complex as precursors in aqueous solution. No foreign reducing agents and stabilizing agents were required in the proposal, so as to ensure the purity of Cu_2O@Ag yolk-shell interfaces. Scheme 1 illustrates introducing $[Ag(NH_3)_2]^+$ ions is our key step in producing Ag shell directly onto Cu_2O surface without any other chemical. Here we synthesized complex 26-facet polyhedron Cu_2O with different particle sizes as desirable sacrificial templates in following experiments. In this paper, a series of counterpart experiments under different conditions were operated to investigate Ag-shell formation with controlling template. According to the results, the mechanism of the formation of Cu_2O@Ag yolk-shell composite and Ag cage was deduced. The introduced $[Ag(NH_3)_2]^+$ played a critical role in the formation of perfect Cu_2O@Ag yolk-shell composite and Ag cage. Furthermore, SEM, XRD, and HRTEM confirmed that morphologies of the obtained Cu_2O@Ag yolk-shell composites and Ag cages by in site epitaxial assembly method in the assistance of ammonia group and the self-assembly of Ag nanoparticles were similar to that of Cu_2O template.

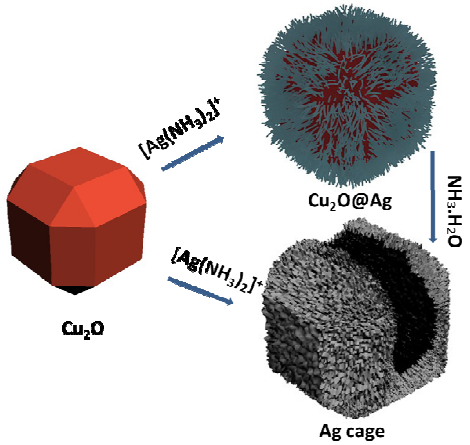

Scheme 1 Illustration of the processing for preparation of Cu_2O@Ag yolk-shell composite and Ag cage under visible-light irradiation in air.

Fig.1 shows a typical scanning electron microscopy (SEM) image of the as-prepared Cu_2O particles synthesized by reducing the copper acetate with ascorbic acid according to the method reported by Wang *et al.* [37] The morphology could be identified as 26-facet polyhedron

Cu_2O whose surface was smooth and particle sizes ranged from 0.4 to 3.5 μm. CA_1 was obtained in the aliquot conversion between Cu_2O and $[Ag(NH_3)_2]^+$, whose molar ratio was 10:1 under 500W Xenon lamp irradiation at room temperature.

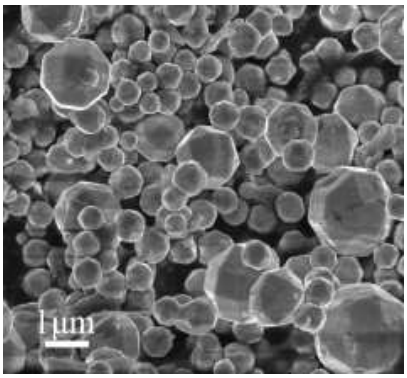

Fig. 1 SEM image of 26-facet polyhedron Cu_2O.

Fig. 2 a-c show the SEM of the CA_1 in different magnifications. It is noteworthy that the surface of the Cu_2O particles was fully coated with Ag thorns to form a whole shell. The HRTEM image shows the detail information and interior structure of the composite. The thickness of the Ag shell is approximately 100 nm as shown in Fig. 2d. Ag shell firmly attached to the surface of Cu_2O particles (a strong contrast between their edges (bright) and centres (dark)).

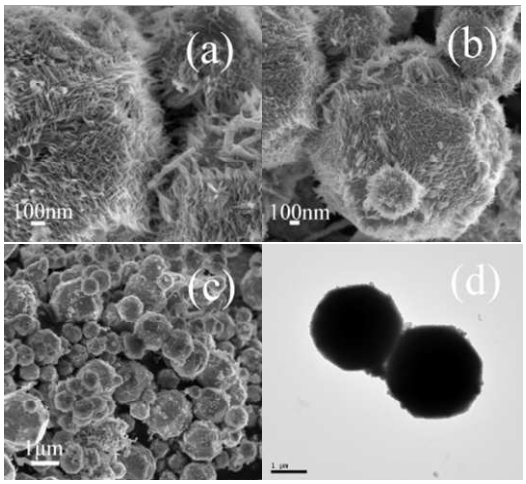

Fig. 2 Morphology information of CA_1. a)-c) are high magnification images of Cu_2O@Ag yolk-shell composite formed by reaction of Cu_2O with $[Ag(NH_3)_2]^+$ (molar ratio was 10:1) under 500W Xenon lamp irradiation in air; d) TEM image of Cu_2O@Ag yolk-shell composite.

The experiment was performed with 1:1 molar ratio between Cu_2O and $[Ag(NH_3)_2]^+$ under the same condition as CA_1. Ultimately, Cu_2O were exhausted and $[Ag(NH_3)_2]^+$ ions were reduced to form Ag cages with large size particles and even lamella (showing as in Fig. 3a-c) in different zones and magnifications. Fig. 3d provided insight of Ag cage morphology similar to that of Cu_2O template, which highlights the role of $[Ag(NH_3)_2]^+$ in the synthesis processing. It is worth noting that sufficient $[Ag(NH_3)_2]^+$ complex adhered to surface of the Cu_2O leading to a complete conversion and formed Ag cage. Employed ultrasonic broken these Ag cages when preparing SEM samples.

XRD analysis was used to determine the phases of pure Cu_2O and the products of CA_1 and CA_2. As seen in Fig. 4a, all the diffraction peaks are in good agreement with the phase of Cu_2O (JCPDS, card No. 05-0667) since 2θ of six peaks are 29.6, 36.5, 42.4, 61.5, 73.6, and 77.4º corresponding to (110), (111), (200), (220), (311), (222), respectively. In Fig. 4c, all the diffraction peaks of CA_2 can ascribe to JCPDS, card No. 04-0783 since 2θ of six peaks are 38.0, 44.3, 64.4, and 77.7º, which are indexed to (111), (200), (220), (311) of Ag, correspondingly. The Fig. 4b shows the XRD pattern of the CA_1, formed by the reaction of Cu_2O with $[Ag(NH_3)_2]^+$ (with 10:1 molar ratio) under 500W Xenon lamp irradiation in air which consisted of the standard spectra of Cu_2O (JCPDS, card No. 05-0667) as yolk and monoclinic Ag (JCPDS, card No. 04-0783) as shell not only in positions, but also in relative intensity. The results means insufficient $[Ag(NH_3)_2]^+$ complex caused aliquot conversion to Cu_2O@Ag yolk-shell under 500W Xenon lamp illumination in air. When the sufficient $[Ag(NH_3)_2]^+$ was used, Cu_2O was exhausted completely and $[Ag(NH_3)_2]^+$ ions were converted to epitaxial assembly Ag cage. Interestingly, Ag cage kept the morphology of Cu_2O perfectly. The preparation process would be deduced as Cu_2O-engaged redox etching as Fig. S1 in SI. Fig. S1a shows the wholesome Cu_2O@Ag yolk-shell, while the shadow in Fig. S1b suggests the existing Cu_2O, consequently, Fig S1c-d, Cu_2O was exhausted and Ag cage formed for sufficient $[Ag(NH_3)_2]^+$ ions.

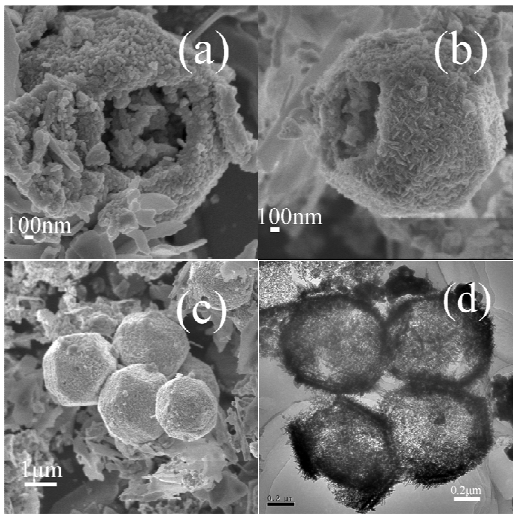

Fig. 3 a) – c) SEM images of CA_2 in different magnifications. CA_2 (Ag cage) formed by reaction of Cu_2O with $[Ag(NH_3)_2]^+$ (molar ratio was 1:1) under 500W Xenon lamp irradiation in air. d) TEM image of CA_2.

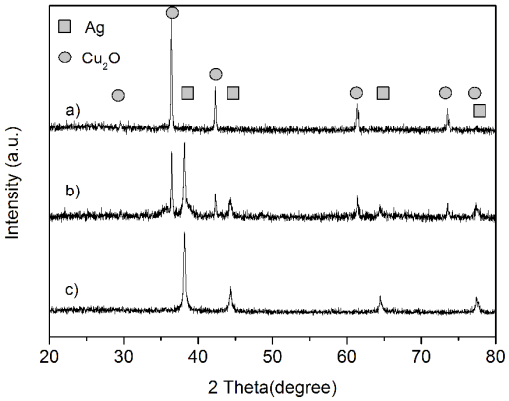

Fig. 4 Typical powder XRD patterns: a) 26-facet Cu_2O; b) the CA1, formed by reaction of Cu_2O with $[Ag(NH_3)_2]^+$ (molar ratio was 10:1) under 500W Xenon lamp irradiation in air; c) the CA_2, formed by reaction of Cu_2O and $[Ag(NH_3)_2]$+ (molar ratio was 1:1) under 500W Xenon lamp irradiation in air.

To study the role of introduced 500W Xenon lamp in the processing. In dark, CA_3 was synthesized by reaction of Cu_2O with $[Ag(NH_3)_2]^+$ ions (molar ratio was 10:1). Fig. S2 in SI shows aliquot

conversion to form Cu_2O@Ag yolk-shell. Ag thorns were fully covered the smooth surface of Cu_2O, while the thickness of the shell is shorter than that of CA_1. So under the 500W Xenon lamp irradiation, the triggered electron accelerate reducing $[Ag(NH_3)_2]^+$ ions to Ag and the Ag growth rate along the thorn direction. XRD pattern of CA_3 in Fig. S4 also confirmed that metal Ag fully covered the surface of Cu_2O and formed Cu_2O@Ag yolk-shell, as the mechanism we deduced.

To investigate the critical role of formed $[Ag(NH_3)_2]^+$ ions, the reaction of the Cu_2O with Ag^+ ions (from $AgNO_3$) under 500W Xenon lamp irradiation without ammonia assistant was performed. Fig. S3 in SI perform the Ag-doped-Cu_2O was formed rather than whole shell. XRD patterns (As Fig. S4 in SI) and SEM (Fig. S3 in SI), the Ag particles were sporadically located on the surface of Cu_2O. Obviously, $[Ag(NH_3)_2]^+$ ions play a pivotal role in the formation of the Cu_2O@Ag yolk-shell composite and Ag cage. Irradiation resource was not indispensable but could promote the growth of Ag. Triggered electron and hole accelerate the redox reaction of Equation 1 and 3.

At the same time, Cu_2O@Ag yolk-shell composites (CA_1) samples were immersed in ammonia aqueous solution (12 wt%) for 30 min with magnetic stirring to extract Cu_2O core of the composite, then obtained CA_5, reacting as Equ. 1.

Fig. 5a-b show the CA_5 is 26-facet cage with thorn-composed shell. In Fig. 5c, strong contrast between their edge (dark) and centre (bright) confirms the Ag cages consist of thorns with 5 nm diameter and 100 nm length. Fig. 5d displays thorns with the lattice distance of 0.2359 nm is Ag shell. The TEM image further reveals that the high-quality single crystals shell with high specific surface areas, rough surface, low densities, hollow interiors, and porous walls.

Fig. 6 displays the low-temperature N_2 adsorption-desorption isotherms of Cu_2O, Cu_2O@Ag yolk-shell, and Ag cage. Characteristic type-IV isotherms are observed, with a type H1 hysteresis loop according to Brunauer-Deming-Deming-Teller (BDDT) classification. The hysteresis loop at high relatively pressure associated with capillary condensation of gases shows the size of mesopores range 2-50 nm. In CA_1 (Cu_2O@Ag yolk-shell) curves, that the formed loop is around 0.8 P/P_0 means macropores have been formed. Meanwhile, that of CA_2 (Ag cage) is around 0.4-0.8 P/P_0, which means Ag cage is composed of both mesoporous and macropores.[38] Due to the hollow and porous structure, the BET specific surface area of the as-prepared Cu_2O, Cu_2O@Ag yolk-shell, and Ag cage are 2.76 m^2g^{-1}, 22.8 m^2g^{-1}, and 46.1 m^2g^{-1}, respectively.

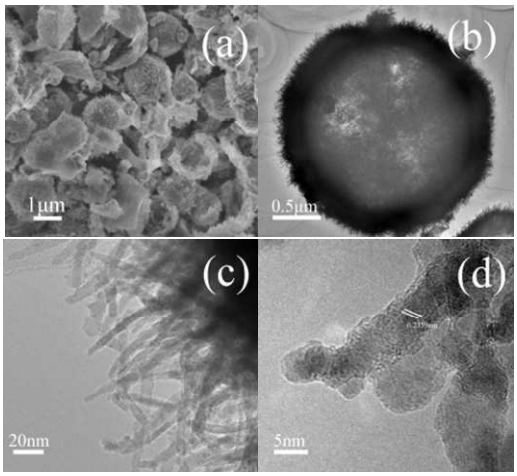

Fig. 5 SEM images of obtained CA_5. a) is high magnification images of formed Ag-cage by immersed CA_1 (Cu2O@Ag yolk-shell composite) into 12wt% ammonia solution; b)-d) are TEM images of the obtained Ag cage.

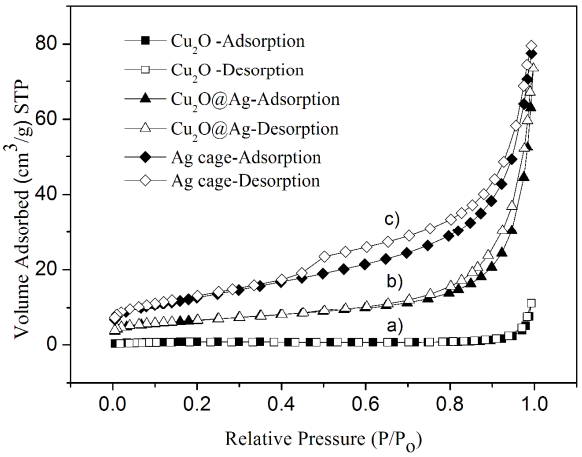

Fig. 6 N_2 adsorption-desorption isotherms of a) Cu_2O; b) Cu_2O@Ag core-shell composite; and c) Ag cage.

From the above discussion, we can deduce the mechanism of in site redox, epitaxial assembly of Cu_2O@Ag and Ag cage is as follows. [39-41]

$$2Cu_2O + 16NH_3.H_2O + O_2(l) \longrightarrow 4[Cu(NH_3)_4]^{2+} + 8OH^- + 12H_2O \quad (1)$$

$$Cu_2O + h\nu \longrightarrow Cu2O^* + e^- + h^+ \quad (2)$$

$$Cu_2O + 2OH^- + h^+ \longrightarrow 2CuO + H_2O \quad (3)$$

$$Ag^+ + e^- \longrightarrow Ag \quad (4)$$

$$Ag^+ + Cu^+ \longrightarrow Cu^{2+} + Ag \quad (5)$$

In summary, we described a versatile synthesis route to synthesize metal Ag on Cu_2O semiconductor in assistance of ammonia solution without any other organic, reductive. Cu_2O@Ag yolk-shell and Ag cage were prepared by using the weakly reductive Cu_2O templates and $[Ag(NH_3)_2]^+$ ions as precursors. It is a novel synthesis method and general rule for epitaxial growth of heterostructure. We believe this method can be used as a new way to prepare high-quality metal-particle-loaded semiconductor composites.

This work was supported by the National High Technology Research and Development Program of China (Grant No. 2012AA063008), the Specialized Research Fund for the Doctoral Program of Higher Education (Grant No. 20100031120029), the National Natural Science Foundation of China (Grant No. 21203102), and Tianjin Key Laboratory of Circular Economy and Low-carbon Development.

Notes and references

Institute of New Catalytic Materials Science and Key Laboratory of Advanced Energy Materials Chemistry (Ministry of Education), College of Chemistry, Synergetic Innovation Center of Chemical Science and Engineering, Nankai University, Tianjin 300071, China. Email: xsliu@nankai.edu.cn; Fax: +86 22-23509005; Tel: +86 22-23509005

†Electronic Supplementary Information (ESI) available: Experimental details and data. See DOI: 10.1039/c000000x/

1 A. A. Herzing, C. J. Kiely, A. F. Carley, P. Landon, G. J. Huntchings, *Science*, 2008, **321**, 1331.
2 J. A. Lopez-Sanchez, N. Dimitratos, C. Hammond, G. L. Brett, L.Kesavan, S. White, P. Miedziak, R. Tiruvalam, R. L. Jenkins, A. F. Carley, D. Knight, C. J. Kiely, G. J. Huntchings, *Nat. Chem.*, 2011, **3**, 551.
3 L. M. C. Pionto, E. Spohr, P. Quaino, E. Santos, W. Schmickler, *Angew. Chem. Inte. Ed.*, 2013, **52**, 7883.

4 H. M. Song, D. H. Anjum, R. Sougrat, M. N. Hedhhili and N. M. Khashab, *J. Mater. Chem.*, 2012, **22**, 25003.
5 G. B. Ingram, S. Linic, *J. Am. Chem. Soc.*, 2011, **133**, 5202.
6 Z. G. Zou, J. H. Ye, K. Sayama, H. Arakawa, *Nature*, 2001, **414**, 625.
7 P. Wang, B. B. Huang, X. Y. Qin, X. Y. Zhang, Y. Dai, J. Y. Wei, M. H. Whangbo, *Angew. Chem. Int. Ed*., 2008, **47**, 7931.
8 C. H. An, S. Peng, Y. G. Sun, *Adv. Mater.*, 2010, **22**, 2570.
9 Y. Q. Qu, R. Chen, Q. Su, X. F. Duan, *J.Am. Chem. Soc.*, 2011, **133**, 16730.
10 J. T. Li, S. K. Cushing, J. Bright, F. K. Meng, T. R. Senty, P. Zheng, A. D. Bristow, N. Q. Wu, *ACS Catal.*, 2013, **3**, 47.
11 F. Hong, S. D. Sun, H. J. You, S. C. Yang, J. X. Fang, S. W. Guo, Z. M. Yang, B. J. Ding, X. P. Song, *Cryst.Growth Des*., 2011, **11**, 3694.
12 B. F. Xin, L. Q. Jing, Z. Y. Ren, B. Q. Wang, H. G. Fu, *J. Phys. Chem. B*, 2005, **109**, 2805.
13 X. Y. Yan, X. L. Tong, Y. F. Zhang, X. D. Han, Y. Y. Wang, G. Q. Jin, Y. Qin, X. Y. Guo, *Chem. Commun*., 2012, **48**, 1892.
14 L. M. C. Pionto, E. Spohr, P. Quaino, E. Santos, W. Schmickler, *Angew. Chem. Inte. Ed.*, 2013, **52**, 7883.
15 J. Khanderi, C. Contiu, J. Engstler, R. C. Hoffmann, J. J. Schneider, A. Drochner, H. Vogel, *Nanoscale*, 2011, **3**, 1102.
16 J.X. Fang, S. Lebedkin, S.C. Yang, H. Hahn, *Chem. Commun.*, 2011, **47**, 5157.
17 Y. Q. Wang, K. Nikitin, D. W. McComb, *Chem. Phys. Lett.*, 2008, **456**, 202.
18 X. Mathew, N. R. Mathews, P. J. Sebastian, *Sol.Energy Mater. Sol.Cells*, 2001, **70**, 277.
19 X. W. Liu, *Langmuir*, 2011, **27**, 9100.
20 A. J. Wang, J. J. Feng, Z. H. Li, Q. C. Liao, Z. Z. Wang, J. R. Chen, *CrystEngComm*, 2012, **14**, 1289.
21 Q. M. Pan, M. Wang, H. B. Wang, J. W. Zhao, G. P. Yin, *Electrochim. Acta*, 2008, **54**, 197.
22 Y. X. Wang, W. Song, J. X. Yang, W. Q. Xu, B. Zhao, *Chem. J. Chinese Universities*, 2011, **32**, 1789.
23 H. X. Su, Z. Chen, *J. Green Sci. and Tec.*, 2013, **3**, 199.
24 X. F. Lin, R. M. Zhou, J. Q. Zhang, S. T. Fei, *Appl. Surf. Sci.*, 2009, **256**, 889.
25 J. H. He, T. Kunitake, *Langmuir*, 2006, **22**, 7881.
26 B. J. Murray, Q. Li, J. T. Newberg, E. J. Menke, J. C. Hemminger, R. M. Penner, *Nano Lett.*, 2005, **5**, 2319.
27 I. I. W. Kim, R. E. Robertson, R. Zand, Cryst. Growth Des., 2005, 5, 513.
28 H.G.Zhang, Q.S.Zhu, Y.Zhang, Y.Wang, L.Zhao, B.Yu,*Adv.Funct.Mater.*, 2007,**17**,2766.
29 J.L.Yu, P.E.Savge, *Appl. Catal. B:Environ.*, 2001,**31**,123.
30A.J.Wang,J.J.Feng,Z.H.Li,Q.C.Liao,Z.Z.Wang, J.R.Chen, *CrystEngComm*, 2012,**14**,1289.
31 P.Poizot, S.Laruelle, S.Grugeon,L.Dupont, J.M.Taracon, *Nature*, 2000,**407**,496.
32A.Paracchino,V.Laporte,K.Sivula,M.Gratzel,E.Thimsen,*Nat.Mater.*,2001,**10**,456.
33 F. Hong, S. D. Sun, H. J. You, S. C. Yang, J. X. Fang, S. W. Guo, Z. M. Yang, B. J. Ding, X. P. Song, *Cryst. Growth Des*., 2011, **11**, 3694.
34 J. F. Pierson, E. Rolin, C. Clement-Gendarme, C. Petitjean, D. Horwat, *Appl. Surf. Sci.*, 2008, **254**, 6590.
35 Z. H. Wang, S. P. Zhao, S. Y. Zhu, Y. L. Sun, M. Fang, *CrystEngComm*, 2011, **13**, 2262.
36 a) G. C. Xi, J. H. Ye, Q. Ma, N. Su, H. Bai, C. Wang, *J. Am, Chem. Soc.*, 2012, **134**, 6508; b) Z.Y.Wang, D.Y.Luan, C.M.Li, F.B.Su. S.Madhavi, F.Y.C.Boey, X.W.Lou, *J. Am, Chem. Soc.*, 2010, **132**, 16271; c) Y. Q. Wang, T. Gao, K. Wang, X. P. Wu, X. J. Shi, Y. B. Liu, S. Y. Lou, S. M. Zhou, *Nanoscale*, 2012, **4**, 7121.
37 X.P.Wang, S.H.Jiao, D.P.Wu, Q.Li, J.G.Zhou, K.Jiang, D.S.Xu, *CrystEngComm*, 2013,**15**,1849.
38 J.G.Yu, J.J.Fan, K.L.Lv, *Nanoscale* 2010,**2**,244.
39 S. H. Jiao, L. F. Xu, K. Jiang, D. S. Xu, *Adv. Mater.* 2006, **18**, 1174.
40 A. E. Rakhshami, *J. Appl. Phys*., 1991, **69**, 2290.
41 C. Sun, Z.X. Yu, B.N. Zhou, S.G. Chen, *Chinese J. Nonferr. Metals*, 1999, **9**, 821.

Manuscript ID RA-COM-03-2014-001805

Title: Ammonia-Assistant Epitaxial Assembly of Cu_2O@Ag Yolk-Shell and Ag Cage

Author(s): Jiqiao Zhang, Cui Zhang, and Shuangxi Liu*

Colour graphic:

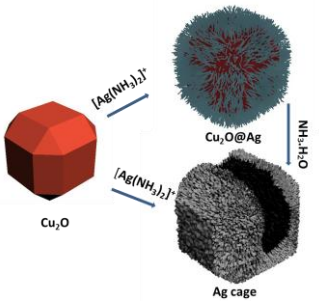

Research Highligh:

Pure Cu_2O@Ag and Ag cage were synthesized by introducing $[Ag(NH_3)_2]^+$ complex to Cu_2O suspension, without any other chemical required.